A Scalable Model for Channel Access Protocols in Multihop Ad Hoc Networks *

Marcelo M. Carvalho
Computer Engineering Department
University of California
Santa Cruz, CA 95064
carvalho@soe.ucsc.edu

J. J. Garcia-Luna-Aceves
Computer Engineering Department
University of California
Santa Cruz, CA 95064
jj@soe.ucsc.edu

ABSTRACT

A new modeling framework is introduced for the analytical study of medium access control (MAC) protocols operating in multihop ad hoc networks. The model takes into account the effect of physical-layer parameters on the success of transmissions, the MAC protocol on the likelihood that nodes can access the channel, and the connectivity of nodes in the network. A key feature of the model is that nodes can be modeled individually, i.e., it allows a per-node setup of many layer-specific parameters. Moreover, no spatial probability distribution or a particular arrangement of nodes is assumed; the model allows the computation of individual (per-node) performance metrics for any given network topology and radio channel model. To show the applicability of the modeling framework, we model multihop ad hoc networks using the IEEE 802.11 distributed coordination function and validate the results from the model with discrete-event simulations in Qualnet. The results show that our model predicts results that are very close to those attained by simulations, and requires seconds to complete compared to several hours of simulation time.

Categories and Subject Descriptors

I.6.5 [**Simulation and Modeling**]: Model Development—*Modeling methodologies*; C.4 [**Performance of Systems**]: Modeling Techniques; C.2.5 [**Local and Wide-Area Networks**]: Access schemes; C.2.1 [**Network Architecture and Design**]: Wireless Communication—*ad hoc networks*

General Terms

Theory, Performance

*This work was supported in part by CAPES/Brazil, by the U.S. Air Force under grant No. F49620-00-1-0330, and by the Baskin Chair of Computer Engineering at UCSC.

MobiCom'04, Sep 26–Oct 1, 2004, Philadelphia, USA.

Keywords

Modeling, ad hoc networks, medium access control, performance evaluation.

1. INTRODUCTION

The medium access control (MAC) protocol of a computer network enables nodes to determine their right to access the available channel(s), while attempting to enforce fair and efficient usage of the channel(s). Establishing such access rights is far more difficult in an ad hoc network than in a wired long haul network or a local area network (LAN), because the radio channels of an ad hoc network are broadcast in nature and radio connectivity is such that the topology of an ad hoc network is not as clearly defined as with point-to-point wire networks. Unlike wired channels that are fairly stationary and predictable, radio channels are extremely random, and connectivity between two nodes depends on many factors, such as the radio frequency in use, power of the transmitters, terrain, antenna type, transmitter/receiver distance, multipath fading, and the like. Furthermore, the quality of a radio link depends on the transmission activity of all other nodes in the entire system, whose aggregate signal powers can severely degrade the signal-to-noise ratio (SNR) at a particular receiver and, consequently, compromise the successful reception of any on-going packet transmission. Last, but not least, thermal and other background noise sources can also contribute to the failure of a packet reception at a given receiver.

Hence, analyzing the performance of a MAC protocol in an ad hoc network must consider the interactions between the physical (PHY) and the MAC layers. In fact, a cross-layer perspective to both analysis and design of multiaccess communications has been brought to attention with recent advances in wireless communications. As pointed out by Gallager [1] and later by Ephremides and Hajeck [2], the fundamental challenge lies in the choice of a proper model that interfaces the physical layer and network layers. Unfortunately, the bulk of the published work on ad hoc networks has focused on the modeling of medium access schemes where ideal channel conditions and unrealistic assumptions are made. Under the argument of separating the issues strictly related to the protocol operation from the issues intrinsically related to the physical layer, few studies have attempted to incorporate physical layer aspects *directly into the behavior of the protocol*, i.e., explicitly modeling the impact of the physical layer on the *dynamics* of the MAC protocol. Perhaps more importantly, no attempt has ever been made to include not only the physical-layer aspects explicitly into the model, but also to include the interdependencies among nodes under a radio-based topology in a multihop ad hoc network. Although convenient for analytical modeling, it is *not* true that only the transmissions from "one hop" neighbors of a node can cause interference at the node.

Because of the limitations of existing analytical models for ad hoc networks, many researchers have opted to study the impact of physical layer on the dynamics of MAC protocols via discrete-event simulations. However, even with such simulation packages as Qualnet, which are designed to scale with the number of nodes in the MANET, obtaining simulation results that are statistically meaningful (by using many seeds) requires hours of simulation time for scenarios corresponding to just a few minutes of simulated time in MANETs with hundreds of nodes with a given choice of physical-layer parameters. This is clearly not a promising approach for researchers to gain insight on the impact of multiple physical-layer parameters on the operation of MAC protocols!

This paper introduces a new modeling framework for *any* MAC protocol operating in multihop ad hoc networks that focuses on the interoperability between the PHY and the MAC layers. In this sense, the model builds up on their ultimate functionalities, which are those of providing a scheduling discipline for nodes to have access to the channel, and guaranteeing that a transmitted frame is correctly received. To account for the effects of both cross-layer interactions and the interference among *all* nodes, a novel linear model is introduced with which topology and physical layer aspects are naturally incorporated in what we define as *interference matrices*. A key feature of the model, which is introduced in Section 3, is that nodes can be modeled individually, i.e., it allows a per-node setup of many layer-specific parameters. Moreover, no spatial probability distribution or pre-arrangement of nodes is assumed. On the contrary, the model allows the computation of individual (per-node) performance metrics for any given network topology and radio channel model.

Section 2 presents an overview of past work in the modeling and performance analysis of ad hoc networks. Section 4 illustrates the applicability of the new modeling framework by applying it to the well-known IEEE 802.11 distributed coordination function (DCF). In doing so, new analytical results are derived that extend our prior work on fully-connected networks [3], and the work by Bianchi [4]. Section 5 validates the results obtained with the new modeling framework using the Qualnet v3.5 simulation package [5], and demonstrates that the new framework produces results that correlate quite nicely with the results obtained using simulations, and accomplishes this in seconds or fractions of a second, representing five or six orders of magnitude in time savings with respect to the time needed to run the simulations. Following that, Section 6 presents an example of how the new modeling framework can be used for a fast and efficient performance evaluation of multihop ad hoc networks. Finally, Section 7 presents our final remarks and conclusions.

2. RELATED WORK

The bulk of the analytical modeling of wireless ad hoc networks has concentrated on the analysis of MAC protocols in fully-connected segments of networks (e.g., satellite networks, cellular networks, or single-hop wireless LANs (WLANs)), because they are simpler to analyze than multihop networks. The majority of this work has followed the formalism and assumptions introduced by Abramson [6, 7] for the analysis of the ALOHA protocol, and by Tobagi and Kleinrock [8, 9] for the analysis of the carrier sense multiple access (CSMA) protocol. The model typically adopted assumes that all nodes have infinite buffers and transmissions are scheduled according to *independent* Poisson point processes. This implies that packets which were either inhibited from being transmitted or were unsuccessfully transmitted are rescheduled after a "sufficiently long" randomized time out to preserve the Poisson property (i.e., no correlation between new packet arrivals and their rescheduling). Packet lengths are exponentially distributed and are independently generated at each transmission attempt (including retransmissions). In many cases, acknowledgments are assumed to happen instantaneously or, in cases where propagation delay is taken into account, acknowledgment traffic is simply ignored, and periods of collisions are restricted to the propagation time, after which all other nodes are able to perceive any activity in the channel (through the single-hop and perfect-channel assumptions). Regarding the quality of the radio links, they are generally considered error free, and the event of unsuccessful transmission is restricted to packet collisions at the receiver. Examples where such assumptions have been made include [10], [11], [12], [13], [14], [15], [16], and [17].

Other works consider physical-layer aspects more explicitly within the context of single-hop scenarios. Raychauduri [18] analyzed slotted ALOHA with code division; Gronemeyer and Davis [19] considered spread-spectrum slotted ALOHA with capture due to time of arrival. Musser and Daigle [20] derived the throughput of pure ALOHA with code division. Pursley [21] studied the throughput of frequency-hopped spread-spectrum communications for packet radio networks. In other cases, the error-free link assumption was relaxed and multipath fading channels where considered while preserving other original assumptions (e.g., Poisson scheduling). This is the case in the works by Arnbak and Blitterswijk, who studied the capacity of slotted ALOHA in Rayleigh-fading channels [22].

More recently, with the advent of the IEEE 802.11 standard for WLANs, a significant amount of work has been carried out to provide an analytical model for its operation. Unfortunately, the vast majority of this effort has considered only single-hop networks under ideal channel conditions [3], [4], [23], [24], [25]. As far as imperfect channel conditions is concerned, Hadzi-Velkov and Spasenovski [26, 27] have investigated the impact of capture on the capacity of the IEEE 802.11 in both Rayleigh- and Rician-fading channels. However, no provision was made to consider a multihop ad hoc network and the interdependencies among the nodes.

Gitman [28] published what is arguably the first paper that actually dealt with a multihop system. Gitman considered a two-hop centralized network consisting of a large number of terminals communicating with a single station via some repeaters located around the station. Subsequently, Tobagi [29, 30] considered the same topology to compute the network capacity and throughput-delay characteristics of both slotted ALOHA and CSMA. However, it was not until the work by Boorstyn et al. [31] that a methodology for the steady-state throughput analysis of a multihop packet radio network was introduced. Based on assumptions like independent Poisson scheduling at each node, exponentially-distributed packet lengths, zero propagation delay, and instantaneous acknowledgments, Boorstyn et al. were able to represent a CSMA multihop network as a continuous-time Markov chain, with the state at each time being the set of transmitting nodes. This analysis lead to a product-form solution and an iterative procedure was used to obtain the scheduling rates corresponding to given desired link traffic rates. The complexity of the algorithm by Boorstyn et al., although exponential in general, grows quadratically or cubically with the *number of links* for most networks on the order of 100 nodes. Tobagi and Brazio [32] considered the same model and observed that it is applicable to ALOHA and C-BTMA (a variant of BTMA). They also observed that not all schemes could be modeled by simply tracking the set of transmitting nodes. Shepard [33] considered fundamental physical-layer aspects in the modeling of large, dense packet-radio networks. Although Shepard's model considered aspects closer to the underlying physics of radio communications, it did not target the modeling of the interaction among the nodes and their interdependencies.

Chhaya and Gupta provided one of the first analytical models of the IEEE 802.11 DCF that considered a multi-hop scenario and where both capture and hidden terminals were taken into account [34]. Like prior work, however, all nodes were assumed to transmit independently according to some Poisson point process. Moreover, in their numerical results, they considered that *all* individual scheduling processes offered the *same load*, regardless of network topology, therefore ignoring the many interdependencies among nodes and their impact on individual scheduling rates. Subsequently, Wang and Garcia-Luna-Aceves [35] provided a model for the saturation throughput of collision avoidance protocols that included the IEEE 802.11 DCF. Their modeling approach is based on the work by Wu and Varshney [36], in which nodes are spatially distributed according to a two-dimensional Poisson distribution, and two Markov models are used to represent the channel around a node and its activity. To obtain the Markov models, the channel is modeled as a circular region in which nodes within the region can communicate with each other, while weak interactions are assumed with nodes outside this region.

Another important venue of research emerged in the last few years that focuses on the problem of *network capacity*. The main objective of this line of work consists of finding fundamental limits on achievable communication rates in wireless networks. In such a problem formulation, a set of rates between source-destination pairs is called achievable if there exists a network control policy that guarantee those rates. The closure of the set of achievable rates is the capacity region of the network. In their seminal work, Gupta and Kumar [37] considered a joint optimization of transmission powers and schedules, showing that the maximum per-node throughput scales proportionally to $1/\sqrt{n}$, where n is the number of nodes. Subsequent works have studied network capacity from various viewpoints (e.g., [38, 39, 40, 41, 42, 43]) while others considered the joint optimization of resource allocation and scheduling [44, 45], or the optimal cross-layer design of PHY and MAC layers [46, 47]. Despite the undeniable importance of such studies, a gap still remains on the modeling of wireless ad hoc networks under *specific* (optimally designed or not) MAC and PHY layers, in a way that the impact of their interactions and the interdependence among the nodes in a multihop environment are all taken into account in the performance evaluation of each node.

3. THE ANALYTICAL MODEL

Our analytical model focuses on the essential aspects of the PHY and MAC layers, as well as their interaction. On the one hand, the MAC layer provides a scheduling discipline for nodes to access the shared channel(s) of the network, and this discipline renders probabilities that nodes will attempt to transmit. On the other hand, the PHY layer encodes information attempting to ensure that the transmitted frames are received correctly; the likelihood with which a transmission is successful depends on how well the signaling used defends against channel impairments and interference from any source. Clearly, the dynamics of the MAC layer is tightly connected to the dynamics of the PHY layer! This interaction between PHY and MAC layers is a function of the connectivity of nodes in the ad hoc network, which is not a deterministic boolean function, but rather a function of the location of nodes, their transmission and sensing ranges, and other factors that together determine the *topology* of the network. Accordingly, the performance experienced by a node is a complex function of the signals used at the PHY layer, the scheduling established at the MAC layer, and the topology of the network.

In the sequel, we build our modeling framework by expressing each layer's functionality in probabilistic terms, i.e., in the PHY layer we are concerned with the probability of a successful frame transmission, whereas in the MAC layer we are concerned with its scheduling rate (transmission probability). We model the interaction between a node and every other node in the network by means of interference matrices.

3.1 Impact of the PHY Layer: Successful Frame Reception Probability

The quality of the radio link between any two nodes in an ad hoc network may vary considerably over time, even in the case when the two nodes are within range of each other. The time-variant nature of a radio link is due to physical layer aspects, as well as the transmission activity of all other nodes in the network, which is controlled by the MAC scheme. Individually, a node's transmission may not interfere with some packet reception at a distant node. However, collectively, the aggregate interference from many simultaneous transmissions might do.

With few exceptions (e.g., [48, 49]), most prior models of MAC protocols assume that all packets received at the same time by a receiver "collide" and, therefore, are destroyed. This assumption is reasonable if the powers of the received signals are nearly the same. In most situations, however, the powers of the received signals are subject to large-scale path loss propagation, shadowing, and small-scale multipath fading [50]. Even when packets from different nodes overlap in time, it may still be possible to successfully decode the packet with the strongest received signal strength—the so-called capture phenomenon [51]. Moreover, a number of choices in system design at the PHY layer have a direct impact on the successful reception of a packet by a given receiver.

For all the above considerations, a link in a wireless ad hoc network may generally be seen as an *asymmetric* channel, and the conditions for a packet to be successfully received at one end of the link may be significantly different at the other end. Therefore, we need to consider network topology in a broader sense, in which asymmetries, unpredictability, and physical-layer aspects are explicitly incorporated into the model.

For the purposes of this paper, we classify the channel signaling methods into two types [52]: *narrowband* and *spread-spectrum* systems. In narrowband signaling, data bits are modulated directly onto the carrier. On spread-spectrum systems, some form of coding is used to get a much wider bandwidth than narrowband schemes do for the same data rate. In many cases, spread-spectrum signaling is the signaling method of choice because of its anti-jamming capabilities, robustness to multi-path effects, lower power spectrum density, and potential for multiuser access through CDMA techniques, i.e., the use of orthogonal codes that can overlap in time with little or no effect on each other. As an example, the IEEE 802.11 standard supports both direct sequence spread spectrum (DSSS) and frequency-hopped spread spectrum (FHSS) systems [53].

In this paper, we assume a direct sequence spread spectrum ad hoc network. In such networks, *multiple access interference* (MAI) plays a major role on network capacity [37], [54]: in the demodulation of each signal, signals from other nodes transmitting simultaneously over the channel appear as interference. The level of such interference varies according to the number of active nodes at any time (dictated by the underlying medium access control scheme). For this reason, not only capacity, but many QoS measures in wireless ad hoc networks are intrinsically dependent on the received *signal-to-interference-plus-noise density ratio* (SINR). More specifically, let V denote the finite set of $|V| = n$ nodes spanning the network under consideration, and $V_r \subseteq V$ the subset of nodes whose signal powers can be perceived at node r *significantly*. In other words, by letting $V_r \subseteq V$ we also consider the cases where there exist nodes in V whose contributions to the aggregate interference at node r are practically neglible because of the RF propagation effects in place. Let now P_k^r denote the received signal power at node r for a signal transmitted by node $k \in V_r$. Then, the signal-to-interference-plus-noise density ratio SINR_i^r for a signal transmitted by node i and received at node r, is given by (using a conventional matched filter receiver) [55]:

$$\mathrm{SINR}_i^r = \frac{P_i^r L_i}{\sum_{j \in V_r, j \neq i} \chi_j P_j^r + \sigma_r^2}, \tag{1}$$

where L_i is the spreading gain (or bandwidth expansion factor) of the spread-spectrum system, σ_r^2 is the background or thermal noise power at the front end of the receiver r, and χ_j is an on/off indicator, i.e.,

$$\chi_j = \begin{cases} 1, & \text{if } j \text{ transmits at the same time,} \\ 0, & \text{otherwise.} \end{cases} \tag{2}$$

In Eq. (1), it is assumed that nodes use long, orthogonal pseudo-random sequences [55], and that the thermal and background noise is modeled as a white Gaussian noise process. The same assumptions are used in such simulators as Glomosim, Ns-2, and Qualnet [5].

Each time node i transmits a frame to node r, the (instantaneous) MAI level at node r depends on the nodes in V_r that are transmitting concurrently with node i, as indicated by the variable χ_j, which is Bernoulli-distributed with probability τ_j, *the probability that node j transmits a frame at any time, according to the MAC protocol in place.*

If $|V_r| = n_r$, there are exactly $2^{n_r - 1}$ combinations of active transmitting nodes (*interferers*) in V_r, excluding the transmitter i itself. In what follows, let $\{c_{ik}^r\}_{k=1,\dots,2^{n_r-1}}$ denote the set of such combinations, and $\mathcal{C}_i^r$ be a random variable that indicates the occurrence of a specific combination c_{ik}^r of interferers.

For simplicity, we assume that, when node i transmits a frame to node r, the set of interferers remain the same throughout the entire transmission of the frame. In reality, of course, some nodes may become active or inactive during the course of a frame transmission. However, this assumption is reasonable if frames are short and transmission rates are high. Consequently, during the reception of a frame, and for a *fixed* set of interferers, the bit-to-bit variations that may occur in SINR_i^r will result from RF propagation effects only. Typically, the received signal powers $P_k^r,\ k \in V_r$, are subject to large-scale path loss , shadowing, and small-scaling multipath fading [50].

Given the considerations above, the probability q_i^r *that a frame transmitted by i is successfully received at r* can be obtained by considering the set $\{c_{ik}^r\}_{k=1,\dots,2^{n_r-1}}$ of all possible combinations of active nodes in V_r, as follows:

$$\begin{aligned} q_i^r &= P\{\text{ successful frame reception }\} \\ &= \textstyle\sum_k P\{\text{ successful frame reception}, \mathcal{C}_i^r = c_{ik}^r\} \\ &= \textstyle\sum_k P\{\text{ succ. frame reception} \,|\, \mathcal{C}_i^r = c_{ik}^r\} P\{\mathcal{C}_i^r = c_{ik}^r\} \\ &= \textstyle\sum_k f(c_{ik}^r) P\{\mathcal{C}_i^r = c_{ik}^r\}, \end{aligned} \tag{3}$$

where we wrote $f(c_{ik}^r)$ to emphasize the fact that $P\{$succ. frame reception $\mid \mathcal{C}_i^r = c_{ik}^r\}$ is a function of the specific combination c_{ik}^r of interferers. Its functional form will depend on the specific choice of radio channel model and such PHY-layer aspects as modulation and demodulation schemes, channel coding, receiver design, and the like.

The above formalism allows for the consideration of *any* radio channel model and PHY-layer aspect for computation of the probability $f(c_{ik}^r)$ of successful frame reception conditioned on a certain MAI level. For instance, one could choose to model the impact of a specific modulation scheme under correlated bit errors during frame reception.

Now, let us consider the probability that the set of active interferers is c_{ik}^r, i.e., $P\{\mathcal{C}_i^r = c_{ik}^r\}$. This probability is a function of the MAC-dependent transmission probabilities $\tau_j,\ j \in V_r$, which, for each node, depends on the perceived activity of other nodes. Hence, assuming that $\tau_j,\ j \in V_r$, is known, we make the simplifying assumption that $P\{\mathcal{C}_i^r = c_{ik}^r\}$ is given by

$$P\{\mathcal{C}_i^r = c_{ik}^r\} = \prod_{m \in \overline{c_{ik}^r}} (1 - \tau_m) \prod_{n \in c_{ik}^r} \tau_n, \tag{4}$$

where $\overline{c_{ik}^r}$ denotes the complement set of c_{ik}^r, i.e., $V_r - \{c_{ik}^r\}$. Finally, from Eqs. (3) and (4),

$$q_i^r = \sum_k f(c_{ik}^r) \prod_{m \in \overline{c_{ik}^r}} (1 - \tau_m) \prod_{n \in c_{ik}^r} \tau_n. \tag{5}$$

3.2 Impact of the MAC Layer: The Transmission Probabilities

So far, we have assumed that a node $k \in V$ transmits a frame according to some scheduling transmission rate (or transmission probability) τ_k dictated by the MAC protocol. In traditional analysis of MAC protocols, the underlying scheduling point process is usually assumed to be Poisson-distributed, and performance evaluation of such MAC protocols are usually conducted by allowing the offered load to vary over a certain range [6], [7], [9], [8], [17]. In these models, it is normally assumed that retransmissions occur after a randomized period in time that is "sufficiently long" in order to preserve the Poisson assumption [7]. By doing so, retransmissions are basically treated as *new transmissions, independent of previous attempts*. Furthermore, in some cases, the packet length of each retransmission is assumed to have been drawn from a given distribution, independent of the original transmission [52].

In reality, when a reliable delivery service is desired at the MAC level, a node retransmits a frame according to some specific rule, until the frame is finally transmitted or discarded after a certain number of failures. At each attempt, if we consider the explicit exchange of frames (ACKs) acknowledging the data frames transmitted, two events need to happen for a node i to consider its frame successfully transmitted to a node r: the successful reception of i's frame at r, and the successful reception of r's acknowledgment at i. Therefore,

$$\begin{aligned} q_i &= P\{\text{DATA successful}, \text{ACK successful}\} \\ &= P\{\text{ACK succ.} \mid \text{DATA succ.}\} P\{\text{DATA succ.}\} \\ &= q_i^r q_r^i = \textstyle\sum_k f(c_{ik}^r) P\{\mathcal{C}_i^r = c_{ik}^r\} \sum_l f(c_{rl}^i) P\{\mathcal{C}_r^i = c_{rl}^i\} \\ &= \textstyle\sum_k \sum_l f(c_{ik}^r) f(c_{rl}^i) P\{\mathcal{C}_i^r = c_{ik}^r\} P\{\mathcal{C}_r^i = c_{rl}^i\} \end{aligned} \quad (6)$$

The MAC protocol dynamically adjusts its behavior according to the feedback that is acquired during its attempts to transmit a particular frame. The MAC protocol must use the feedback information to schedule future retransmissions in a way that minimizes the number of unsuccessful transmissions. In this sense, MAC protocols can be seen as dynamic systems whose feedback information are the successful transmission probabilities q_i and the corresponding outputs are the scheduling rates $\tau_i,\ i \in V$. Therefore, the MAC operation can be represented by some function $h_i(\cdot)$ that maps the feedback input into the desired outputs, which are the scheduling rates. We use the subscript i in the mapping function $h_i(\cdot)$ to denote a node-specific MAC-protocol output.

Strictly speaking, the MAC operation should be seen as a time-variant system, where probabilities should also be time-variant (a stochastic process). However, we will assume that, in the long-run (or in steady-state), the operation of the MAC protocol can be represented by a time-invariant (linear or non-linear) function $h_i(\cdot)$ relating the probabilities q_i and τ_i, $i \in V$, i.e.,

$$\tau_i = h_i(q_i),\ i \in V. \quad (7)$$

Notice that, rigorously speaking, τ_i may be a function of not only q_i, but also of the steady-state probability that a packet is available at a node's queue, i.e., that the queue is not empty. Consequently, τ_i should also be a function of the particular input data traffic distribution at node $i \in V$. In the literature, however, the throughput of a packet-radio network is studied by assuming saturation at all nodes, i.e., all buffers are full [52]. In this paper, we also assume that a packet is always available for transmission at the head of a node's queue (being a retransmission or not). For this reason, we can adopt Eq. (7) to represent the steady-state operation of the MAC protocol.

The *coupled nonlinear multivariate system* on the variables τ_i and $q_i,\ i \in V$, represented by Eqs. (4), (6), and (7), allows us to consider the interdependence between the PHY layer and the MAC layer explicitly, as well as the interdependence among *all nodes* in the network! However, solving such a nonlinear system in arbitrary topologies constitutes an extremely complex task if we consider the number of possibilities for the functional forms of $f(\cdot)$, $h_i(\cdot)$, and network sizes. Furthermore, checking for the existence of a solution for the system can be very cumbersome, if not impossible. Hence, to simplify our modeling problem and to better understand the effects of different protocol parameters on the probabilities τ_i and q_i, in the next section we *linearize* the above nonlinear system.

3.3 The Impact of Topology: The Linear Model

Let us first consider the probability τ_i that a node transmits a packet at any given time as expressed by Eq. (7). According to our previous remarks, the MAC-dependent functional form $h_i(\cdot)$ may be a linear or non-linear function of the successful transmission probability q_i. To generalize, let us assume that it is a non-linear function. Therefore, if $h_i(q_i)$ is a function with a continuous nth derivative throughout the interval $[0, 1]$, the Taylor series expansion of $h_i(q_i)$ is given by

$$h_i(q_i) = h_i(0) + q_i h_i'(0) + \cdots + \frac{q_i^{n-1}}{(n-1)!} h_i^{(n-1)}(0) + R_n, \quad (8)$$

where $R_n = \frac{q_i^n}{n!} h_i^{(n)}(\epsilon), \quad 0 \le \epsilon \le q_i$.

Let $h_i(q_i)$ be a function such that $h_i(0) \approx 0$, i.e., the probability that node i attempts to transmit a packet is nearly zero when, in the long-run, $q_i = 0$. Such situation arises, for instance, in the reasonable case where the MAC behavior (represented by the function $h(\cdot)$) is such that it does not schedule transmissions (i.e., its transmission probability is almost zero) if it knows that packets will not be delivered (from the "feedback information" $q_i = 0$). In this case, a first-order approximation for $h_i(q_i)$ is simply

$$\tau_i = h_i(q_i) \approx a q_i, \quad \text{where} \ \ a = h_i'(0), \quad (9)$$

which, considering all nodes in the topology, can be rewritten in matrix notation as follows:

$$\boldsymbol{\tau} = a\mathbf{q}, \quad (10)$$

where $\boldsymbol{\tau} = [\tau_1\ \tau_2\ \ldots\ \tau_n]^T$ and $\mathbf{q} = [q_1\ q_2\ \ldots\ q_n]^T$.

Let us now consider the probability q_i that a successful transmission occurs. According to Eq. (6), q_i depends on a number of terms involving the transmission probabilities τ_j, as given by Eq. (4). When contention among nodes is high, τ_j is expected to be generally small. In addition, because the conditional probability of successful frame transmission $f(\cdot)$ decreases as the MAI level increases (the SINR deteriorates), the term in the double summation of Eq. (6) that contributes the most to the computation of q_i is exactly the one that corresponds to the case when *none* of the potential interferers of nodes i and r transmit, i.e., the MAI is null. In this case, all terms in the products of Eq. (4) will be of the form $(1 - \tau_m)$, and the SINR will be the highest possible, maximizing $f(\cdot)$. If we let c^r_{i0} and c^i_{r0} denote the combinations corresponding to the case when *no* interferer of both r and i transmit, i.e., $c^r_{i0} = c^i_{r0} = \{\emptyset\}$, meaning that $\overline{c^r_{i0}} = V_r$ and $\overline{c^i_{r0}} = V_i$, then we can approximate q_i as follows:

$$\begin{aligned} q_i &= \sum_k \sum_l f(c^r_{ik}) f(c^i_{rl}) P\{\mathcal{C}^r_i = c^r_{ik}\} P\{\mathcal{C}^i_r = c^i_{rl}\} \\ &\approx f(c^r_{i0}) f(c^i_{r0}) P\{\mathcal{C}^r_i = c^r_{i0}\} P\{\mathcal{C}^i_r = c^i_{r0}\} \\ &= f(c^r_{i0}) f(c^i_{r0}) \prod_{j \in V_r} (1 - \tau_j) \prod_{k \in V_i} (1 - \tau_k), \end{aligned} \quad (11)$$

From Eq. (9),

$$q_i = f(c^r_{i0}) f(c^i_{r0}) \prod_{j \in V_r} (1 - a q_j) \prod_{k \in V_i} (1 - a q_k). \quad (12)$$

If we assume $a << 1$, and because $0 \leq q_i \leq 1$, we can approximate the previous products as follows:

$$\begin{aligned} q_i &\approx f(c^r_{i0}) f(c^i_{r0}) \left(1 - a \sum_{j \in V_r} q_j\right) \left(1 - a \sum_{k \in V_i} q_k\right) \\ &\approx f(c^r_{i0}) f(c^i_{r0}) \left(1 - \sum_{j \,\in\, V_r \cup V_i} a q_j\right). \end{aligned} \quad (13)$$

Now, making $f(c^r_{i0}) f(c^i_{r0}) = \pi_i$, and considering the set V of all nodes in the network, with r_i denoting the intended receiver of node i, we have that

$$q_1 = \pi_1 - a\pi_1 \sum_{j \in V_{r1} \cup V_1} q_j \quad (14)$$

$$q_2 = \pi_2 - a\pi_2 \sum_{j \in V_{r2} \cup V_2} q_j \quad (15)$$

$$\vdots$$

$$q_n = \pi_n - a\pi_n \sum_{j \in V_{r_n} \cup V_n} q_j. \quad (16)$$

which, in matrix notation becomes

$$\begin{bmatrix} q_1 \\ q_2 \\ q_3 \\ \vdots \\ q_n \end{bmatrix} = \begin{bmatrix} \pi_1 \\ \pi_2 \\ \pi_3 \\ \vdots \\ \pi_n \end{bmatrix} - \begin{bmatrix} 0 & \phi_{12} & \phi_{13} & \cdots & \phi_{1n} \\ \phi_{21} & 0 & \phi_{23} & \cdots & \phi_{2n} \\ \phi_{31} & \phi_{32} & 0 & \cdots & \phi_{3n} \\ \vdots & \vdots & \vdots & \ddots & \vdots \\ \phi_{n1} & \phi_{n2} & \phi_{n3} & \cdots & 0 \end{bmatrix} \begin{bmatrix} q_1 \\ q_2 \\ q_3 \\ \vdots \\ q_n \end{bmatrix}, \quad (17)$$

where

$$\phi_{ij} = \begin{cases} a\pi_i, & \text{if } j \in V_i \cup V_{r_i} \\ 0, & \text{if } j \notin V_i \cup V_{r_i} \end{cases} \quad (18)$$

Or, in a more compact form,

$$\mathbf{q} = \boldsymbol{\pi} - \mathbf{\Phi}\mathbf{q}, \quad (19)$$

leading to the linear system

$$(\mathbf{I} + \mathbf{\Phi})\mathbf{q} = \boldsymbol{\pi}, \quad (20)$$

where $\mathbf{I}$ is the identity matrix, $\mathbf{\Phi}$ is the $n \times n$ matrix in Eq. (17), and $\boldsymbol{\pi} = [\pi_1\, \pi_2 \ldots \pi_n]^T$. In its essence, the matrix $\mathbf{\Phi}$ conveys all the information regarding how each node interferes with every other node in the network based on the effect of the PHY and MAC layers. For this reason, we refer to $\mathbf{\Phi}$ as the **interference matrix**.

The linear system in Eq. (20) has a solution if and only if, the vector $\boldsymbol{\pi}$ is in the column space of the matrix $\mathbf{\Psi} = \mathbf{I} + \mathbf{\Phi}$, i.e., it is a linear combination of the columns of $\mathbf{\Psi}$. Given the generality of the matrix $\mathbf{\Psi}$, which can change every time we consider a different network topology (through the interference matrix $\mathbf{\Phi}$), we need to find out which matrices $\mathbf{\Psi}$ allow the linear system of Eq. (20) to have a solution. In fact, we will aim higher and ask, ultimately, if the system of Eq. (20) has a solution *regardless of network topology.* Indeed, the answer to this question is *yes* and is the result of Theorem 1 below.

DEFINITION 1. *A square matrix* $\mathbf{A}$ *is* **diagonally dominant** *if the absolute value of each diagonal element is greater than the sum of absolute values of the non-diagonal elements in its row. That is,*

$$\sum_j |a(i,j)| < |a(i,i)|, \quad j \neq i.$$

PROPERTY 1. *If the diagonal elements of a square matrix* $\mathbf{A}$ *are all positive and if* $\mathbf{A}$ *and* $\mathbf{A}^T$ *are both diagonally dominant, then* $\mathbf{A}$ *is positive definite.*

THEOREM 1. *Given* $n > 1$, *if* $a < (n-1)^{-1}$ *the matrix* $\mathbf{\Psi} = \mathbf{I} + \mathbf{\Phi}$ *is nonsingular regardless of network topology.*

PROOF. By construction, the diagonal elements of $\mathbf{\Psi}$ are all positive (all ones). In this case, for the matrices $\mathbf{\Psi}$ and $\mathbf{\Psi}^T$ to be diagonally dominant, we must have

$$\sum_j \phi_{ij} < 1, \quad \text{for all}\, i \quad \text{and} \quad \sum_i \phi_{ij} < 1, \quad \text{for all}\, j, \quad (21)$$

where ϕ_{ij} are defined according to Eq. (18). Now, let K denote the set of non-zero off-diagonal elements in a specific line or column of $\mathbf{\Psi}$. Because $0 \leq \pi_i \leq 1$, every line or column of $\mathbf{\Psi}$ satisfies

$$\sum_{k \in K} a\pi_k \;\leq\; \sum_{k \in K} a\pi_{\max} \;\leq\; \sum_{k \in K} a \;\leq\; (n-1)a.$$

From the conditions in the inequalities in (21), and by Property 1, it follows that $\mathbf{\Psi}$ is positive definite if $a < (n-1)^{-1}$. Consequently, by the positive definiteness property, $\mathbf{\Psi}^{-1}$ exists and the theorem is true. □

Considering the fact that a is a function of the parameters of the underlying MAC protocol (from the linearization of $h_i(q_i)$), the condition stated in Theorem 1 actually suggests a design rule for choosing "feasible" MAC parameters for a given network of size n. Note that, the condition imposed on a in Theorem 1 refers to the extreme case when all nodes in a network of size n can hear each other and packets are not missed due to physical layer aspects ($\pi_i = 1\ \forall i$), i.e., a fully-connected network under ideal channel conditions. Finally, if we substitute Eq. (20) into Eq. (10) we get the *transmission probability vector* $\boldsymbol{\tau}$, given by

$$\boldsymbol{\tau} = a(\mathbf{I} + \mathbf{\Phi})^{-1}\boldsymbol{\pi}. \quad (22)$$

Observe that, in the worst case scenario, the linear system of Eq. (20) can be computed in up to $O(n^3)$ operations (where n is the number of *nodes*). Depending on the symmetry of the problem, the complexity can be reduced to $O(n)$ [56]. This indicates that our modeling framework is quite scalable with the number of nodes.

4. APPLICATION: MODELING THE IEEE 802.11 DCF

To show how our modeling framework can be applied to the study of MAC protocols operating in ad hoc networks, we apply our model to the analysis of ad hoc networks using the IEEE 802.11 distributed coordination function (DCF).

Recently, we have derived closed-form expressions for the first two moments of a node's service time in a saturated IEEE 802.11 DCF network, as a function of the channel state as perceived by each node [3]. In this model, the state of the channel is conveyed in the form of *channel state probabilities*, and is expressed in terms of three mutually exclusive events: $E_i = \{\text{idle channel}\}$, $E_c = \{\text{collision}\}$, and $E_s = \{\text{successful transmission}\}$, which are the three events that dominate the behavior of the binary exponential backoff algorithm in the IEEE 802.11 DCF. To compute the channel state probabilities, we use the work by Bianchi [4]. Bianchi's work provides a nonlinear system of equations relating the steady-state probabilities that a node transmits a packet at any given time, and the respective collision probability of this packet for the case of a *fully-connected* network under ideal channel conditions (i.e., no hidden terminals, capture, or considerations of the physical layer whatsoever).

In this section, we extend Bianchi's model [4] and our own prior model aimed at fully-connected networks [3] to consider a general multihop ad hoc network using 802.11 DCF under non-ideal channel conditions. For this purpose, we first review the expressions for the average service time and throughput for a saturated ad hoc network we derive in [3]. For the average backoff time, we found that

$$\overline{T}_B = \frac{\alpha(W_{\min}\beta - 1)}{2q} + \frac{(1-q)}{q}\,t_c, \tag{23}$$

where

$$\beta = \frac{q - 2^m(1-q)^{m+1}}{1-2(1-q)}. \tag{24}$$

In the equations above, $W_{\min}$ is the minimum contention window size specified for the backoff operation, m is the standard-defined maximum power used to set up the maximum contention window size, i.e., $W_{\max} = 2^m W_{\min}$, q is the conditional probability of successful handshake (assumed constant), and $\alpha = \sigma p_i + t_c p_c + t_s p_s$, where $\mathbf{p}_i = [p_i^i \; p_c^i \; p_s^i]^T$ is the vector of channel state probabilities for the events that node i can perceive during its backoff operation, with σ, t_s, and t_c being their corresponding average time duration. Given the backoff time characterization, the *average service time* equals

$$\overline{T} = \overline{T}_B + \overline{T_s}, \tag{25}$$

where $\overline{T_s}$ is the average time to successfully transmit a packet at the end of the backoff operation (dependent on the packet size). Finally, since the network is assumed to be saturated, the average throughput per node is simply [1]

$$S = \frac{E\{\text{Data Payload}\}}{\overline{T}}. \tag{26}$$

One of the drawbacks in our model for fully-connected networks [3] is the fact that frames are allowed to backoff *infinitely* in time, as opposed to what is defined in the standard, where retransmission counters limit the number of attempts to transmit a particular frame, after which the frame is dropped. The infinite backoff abstraction makes the model much more tractable, but makes it too conservative, predicting higher service times (and consequently, lower throughputs) than what actually happens in the IEEE 802.11 DCF [3]. Accordingly, we extend our prior work and develop the average service time for the case of a *finite* backoff operation.

We keep our assumption of a constant conditional successful handshake probability q per transmission attempt, i.e., at the end of a backoff stage, the probability of a successful handshake is constant, regardless of the number of previous attempts. We should point out that, later in our development, this constant probability will depend on the *specific receiver*, as expressed in Eq. (6).

Now, let M be the maximum number of times a frame can be retransmitted, i.e., the maximum number of backoff stages a frame can undergo. In this case, we have a *truncated geometric distribution*, given by

$$P\{B = k\} = \frac{(1-q)^{k-1}q}{1-(1-q)^M}, \quad k = 1, 2, \ldots, M, \tag{27}$$

Hence, following our development in [3], the average service time is now given by (omitting intermediate steps, which are straigthforward but tedious):

$$\overline{T}_B = \frac{\alpha W_{\min}}{2}\beta_1 - \frac{\alpha}{2}\beta_2 + \beta_3\,t_c, \tag{28}$$

where

$$\begin{aligned}
\beta_1 &= \frac{A_1 + A_2 + A_3}{1-(1-q)^M} \\
A_1 &= \frac{2q\{1-[2(1-q)]^m\}}{2q-1} - 1 + (1-q)^m \\
A_2 &= \left(2^{m+1}-1\right)(1-q)^m\left[1-(1-q)^{M-m}\right] \\
A_3 &= \frac{2^m\left\{(1-q)^{m+1} - (1-q)^M[1+q(M-m-1)]\right\}}{q} \\
\beta_2 &= \frac{1-(1-q)^M(1+qM)}{q[1-(1-q)^M]} \\
\beta_3 &= \frac{(1-q)-(1-q)^M[1+q(M-1)]}{q[1-(1-q)^M]},
\end{aligned}$$

where the parameters α, m, $W_{\min}$, and t_c are defined as before.

To find the channel probabilities for a general multihop ad hoc network, we use the work by Bianchi [4] as our starting point. Bianchi provided a model to evaluate the saturation throughput of the IEEE 802.11 DCF MAC protocol under the hypothesis of ideal channel conditions, i.e., no hidden terminals and capture. The novelty of his approach comes from the fact that many of the details of the IEEE 802.11 binary exponential backoff algorithm were taken into account when modeling the stochastic process describing the backoff time counter of a given node. To accomplish this, the key assumption adopted in the model was that each frame collided with a constant and independent probability p at each transmission attempt, regardless of the number of retransmissions already occurred. This probability was called the *conditional collision probability*, i.e., the probability of a collision experienced by a frame being transmitted in the channel. In Bianchi's development, a fixed number n of nodes was assumed, with each node always having a packet

[1] For more details, see [3].

available for transmission, i.e., the transmission queue of each node was always nonempty. Then, the probability τ that a node transmits a frame at any time was obtained by modeling the stochastic process representing the backoff time counter as a bidimensional discrete-time Markov process. For convenience, we repeat the expression for τ obtained by Bianchi:

$$\tau = \frac{2(1-2p)}{(1-2p)(W_{\min}+1)+pW_{\min}(1-(2p)^m)}. \tag{29}$$

To model a multihop wireless ad hoc network using the IEEE 802.11 DCF, we need to consider each node individually. As before, let V denote the finite set of $|V| = n$ nodes spanning the network under consideration. Each time a node $i \in V$ attempts to perform a handshake (at the end of a backoff stage) it will experience a failure with probability p_i. As in Bianchi's work, and given that we are not considering mobility, we will also assume that p_i is constant and independent of the number of retransmissions that already occurred (constant with respect to the number of retransmissions, but dependent on the chosen receiver because we are including the physical layer aspects now). In the specific case of single-hop networks under ideal channel conditions, previous models implicitly assumed that a successful reception of an RTS (DATA) frame was sufficient for a successful handshake to occur. However, in the multihop environment under non-ideal conditions, a successful handshake depends on the occurrence of at least two events: the successful reception of both RTS (DATA) and CTS (ACK) frames. As far as the backoff dynamics is concerned, only the reception of RTS and CTS packets determines if a node leaves the backoff state or not. For the moment, we will disregard possible collisions involving DATA packets or ACK control packets in the four-way handshake scheme. For this reason, we will refer to the probability p_i in a more general sense, as the *conditional probability of a failed handshake*. Given p_i and the previous assumptions, the stochastic process governing a node's backoff time counter is well defined and, therefore, its steady state transmission probability τ_i can be expressed in the same way as in Eq. (29), except that it now refers to each node individually:

$$\tau_i = \frac{2(1-2p_i)}{(1-2p_i)(W_{\min}+1)+p_iW_{\min}(1-(2p_i)^m)}. \tag{30}$$

Eq. (30) is exactly what we need to apply our modeling methodology: it gives us the functional form $h_i(q_i)$ by which the MAC layer relates the steady-state transmission probability τ_i with the successful transmission probability $q_i = 1 - p_i$. Therefore, all that is left for us to do is to compute a first order approximation for it. For this purpose, let η_i be the probability that node i *does not* transmit in a randomly chosen slot time, i.e.,

$$\eta_i = 1-\tau_i = \frac{(1-2p_i)(W_{\min}-1)+p_iW_{\min}(1-(2p_i)^m)}{(1-2p_i)(W_{\min}+1)+p_iW_{\min}(1-(2p_i)^m)}. \tag{31}$$

Given the continuity of both $\eta_i(p_i)$ and its derivatives[2] in the interval $p_i \in (0, 1)$, the Taylor series expansion of $\eta_i(p_i)$ at $p_i = 0$ is given by

$$\eta_i(p_i) = \frac{W_{\min}-1}{W_{\min}+1} + \frac{2W_{\min}}{(W_{\min}+1)^2}p_i + O(p_i^2), \tag{32}$$

where $O(p_i^2)$ accounts for the second and high order terms in the Taylor series expansion. Hence, a first order approximation of $\eta_i(p_i)$ is simply

$$\eta_i(p_i) = \frac{W_{\min}-1}{W_{\min}+1} + \frac{2W_{\min}}{(W_{\min}+1)^2}p_i \tag{33}$$

which, in terms of $q_i = 1 - p_i$ becomes

$$\begin{aligned}\eta_i(q_i) &= -\frac{2W_{\min}}{(W_{\min}+1)^2}q_i + \frac{W_{\min}^2+2W_{\min}-1}{(W_{\min}+1)^2} \\ &\approx -\frac{2W_{\min}}{(W_{\min}+1)^2}q_i + 1. \end{aligned} \tag{34}$$

Given that $\tau_i = 1 - \eta_i$, we can finally express τ_i in terms of the probability q_i as follows:

$$\tau_i(q_i) = \frac{2W_{\min}}{(W_{\min}+1)^2}q_i. \tag{35}$$

If we consider all nodes in the topology, Eq. (35) can be rewritten in matrix notation as follows:

$$\boldsymbol{\tau} = a\mathbf{q}, \tag{36}$$

where $\boldsymbol{\tau} = [\tau_1\ \tau_2\ \dots\ \tau_n]^T$, $a = 2W_{\min}/(W_{\min}+1)^2$, and $\mathbf{q} = [q_1\ q_2\ \dots\ q_n]^T$.

We can now deal with the computation of the channel-state probability vector $\mathbf{p}_i = [p_i^i\ p_c^i\ p_s^i]^T$ for every node $i \in V$. For this purpose, we need to consider the *carrier sensing range* during the times a node is sensing the channel. In general, the carrier sensing range of a node is larger than its transmission range. Therefore, because the dynamics of a node in backoff depends on its perceived state of the channel, we need to take into account the carrier sensing range as opposed to the transmission range when computing the channel state probability vector $\mathbf{p}_i$. That said, let R_i denote the set of nodes within the carrier sensing range of node i. At any given time, the probability that there exists some node from R_i transmitting a frame while node i is in backoff is

$$p_{tr}^i = 1 - \prod_{j\in R_i}(1-\tau_j) \tag{37}$$

The probability p_{suc}^i that a transmission within i's sensing range is successful is given the probability that some node in R_i transmits successfully, conditioned on the fact that at least one node in R_i attempted to transmits, i.e.,

$$\begin{aligned} p_{suc}^i &= \frac{\sum_{k\in R_i} P\{k \text{ transmits } \cap\ k \text{ is successful}\}}{p_{tr}^i} \\ &= \frac{\sum_{k\in R_i} P\{k \text{ is successful} \mid k \text{ transmits}\}P\{k \text{ transmits}\}}{p_{tr}^i} \\ &= \frac{\sum_{k\in R_i} q_k\tau_k}{p_{tr}^i} \end{aligned} \tag{38}$$

From Eqs. (37) and (38), the probability p_s^i that a successful transmission occurs within i's sensing range is then $p_s^i = P\{E_s\} = p_{tr}^i p_{suc}^i$. Accordingly, the probability p_i^i that the channel within i's sensing range is idle is simply $p_i^i = P\{E_i\} = 1 - p_{tr}^i$, and the probability p_c^i that a collision

[2] Continuity with respect to the critical value $p = 1/2$ can be shown by simply rewriting $\eta_i(p_i)$ in the same way as it was done for $\tau_i(p_i)$ by Bianchi [4].

occurs within i's sensing range is given by $p_c^i = P\{E_c\} = p_{tr}^i(1 - p_{suc}^i)$.

Finally, we need to know the values of the time intervals t_s and t_c which, for the four-way handshake mechanism, are given by

$$\begin{aligned} t_s &= \text{RTS} + \text{SIFS} + \delta + \text{CTS} + \text{SIFS} + \delta + \text{H} + E\{P\} \\ &\quad + \text{SIFS} + \delta + \text{ACK} + \text{DIFS} + \delta, \\ t_c &= \text{RTS} + \text{DIFS} + \delta. \end{aligned} \tag{39}$$

where $E\{P\} = P$ for fixed packet sizes. Notice that the value of T_s in Eq. (25), is simply $t_s - \text{DIFS}$.

5. MODEL VALIDATION

In this Section, we evaluate the accuracy of our model in predicting the performance of nodes in multihop ad hoc networks using the IEEE 802.11 DCF, focusing on ad hoc networks with static topologies under saturation. Analytical results are compared to numerical simulations using Qualnet v3.5 [5].

5.1 Scenarios Used for Comparison

5.1.1 Radio Channel Model

For the purposes of validation of our modeling framework, we consider a radio channel model with large-scale path loss propagation effects only. We choose a simpler model in order to focus on the model's ability to faithfully represent interdependencies among the nodes and the per-node performance metrics. Nonetheless, as mentioned in Section 3.1, other effects such as shadowing and small-scale multipath fading may be equally taken into consideration when computing the conditional probabilities $f(c_{ik}^r)$ of a successful frame reception in Eq. (3). The path loss propagation model we choose is the two-ray ground reflection model [50].

5.1.2 IEEE 802.11 Parameters

Regarding the IEEE 802.11 PHY layer, we use direct sequence spread spectrum (DSSS) with a raw bit rate of 1 Mbps with DBPSK modulation. Under this configuration, according to the standard, both preamble and MAC protocol data unit (MPDU) are transmitted at the same basic rate, under the same modulation scheme [53]. Without loss of generality, this is done just to ease the analysis and not adding more complexity to the analytical model by treating each segment separately, with different modulation schemes.

Each node has the same transmit power and, for the given path loss propagation model, we select receive and carrier sensing thresholds in a way that the radio range is set to 200 m and carrier sensing range is set to 400 m. Table 5.1.2 summarizes the rest of the parameters used for PHY and MAC layers.

Because multipath fading is not considered, and MAI is disregarded during the approximation of the successful frame reception probability in Eq. (11), bit-to-bit error dependencies are practically null. Hence, the only kind of interference that is left is the thermal and background noise, which is assumed to be white Gaussian noise. Consequently, we can treat bit errors independently, as it is assumed in Qualnet as well. Let $\gamma(c_{i0}^r)$ denote the SINR at node r for a bit transmitted by i when none of r's interferers transmits, i.e., the combination c_{i0}^r, as defined in Section 3.3. If K is the length of the physical layer convergence protocol data unit (PPDU), and $P_b(\gamma)$ is the bit-error probability of DBPSK for a certain SINR level γ, then the conditional probability $f(c_{i0}^r)$ of successful frame reception in Eq. (11) is given by

$$f(c_{i0}^r) = \{1 - P_b[\gamma(c_{i0}^r)]\}^K . \tag{40}$$

Accordingly, the same procedure is used for computation of $f(c_{r0}^i)$ in Eq. (11).

Table 1: IEEE 802.11 Simulation Parameters.

MAC		PHY	
$W_{\min}$	32	Temperature (Kelvin)	290
$W_{\max}$	1024	Noise factor	10
MAC Header (bytes)	34	Transmission power (dBm)	10
ACK (bytes)	38	Sensitiviy of PHY (dBm)	-87.039
CTS (bytes)	38	Minimum power for received packet (dBm)	-76.067
RTS (bytes)	44		
Slot Time (μsec)	20	Packet reception model	BER
SIFS (μsec)	10		
DIFS (μsec)	50		

5.1.3 Interference Matrix Computation

Given the computations of $f(c_{i0}^r)$ and $f(c_{r0}^i)$ as above, one can finally build the linear system of Eq. (20) to compute the transmission probability vector $\boldsymbol{\tau}$ in Eq. (22). For that, we need to know who is the set of interferers for each transmitter/receiver pair, as used in Eq. (13).

Because aggregate MAI is disregarded in the linear model, we select as a potential interferer of a node r any node $j \in V$ whose signal power, when received at r, is above the selected carrier sensing threshold. Any node not conforming to that, we discard as an interferer of r (we would certainly include such signals if MAI were considered and its contribution to aggregate interference were significant). Finally, given the transmission probability vector $\boldsymbol{\tau}$, one can compute the channel state probability vectors $\mathbf{p}_i$ as in Section 4 and, consequently, per-node throughputs according to Eq. (26).

5.1.4 Simulation Setup

Because of the selected radio range, nodes are randomly placed in an area of 1000×1000 m, a size big enough to deploy a multihop network. The only constraint imposed is that the resulting graph is connected. This constraint is added simply to make sure that all nodes have at least one neighbor, and that considerable channel contention and hidden-terminal effects are present in the scenarios.

In simulations, each node chooses the same neighbor node (i.e., a node within its transmission range) for all its transmissions using the same CBR source rate. We pick source rates high enough to saturate all nodes in the network. Packet sizes are fixed to 1500 bytes (IP packet) and each simulation run corresponds to 5 minutes of data traffic. We repeat the experiment for 50 seeds, with each trial corresponding to a different initial transmission time at each node. Initial transmission times are randomly chosen within the interval [0, 0.01] s. This is done to allow the exponential backoff algorithm to be triggered at different instants in time, at each node, so that different state evolutions are taken into account for the same topology.

5.2 Accuracy of Models

Two aspects of interest in our modeling approach are *scalability* and *per-node* performance. To illustrate such aspects, let us consider two network topologies: one with 50 nodes and another with 100 nodes. Figures 1 and 2 show their respective topologies. In the figures, the numbers inside the areas indicate the node ID. To provide an idea of the density of nodes in each topology, a line between two nodes indicates that they are within 200 meters of one another. As it can be observed, the created topologies provide both highly-dense as well as poorly-connected areas. Needless to say, interference at a given receiver in the analytical model and simulations is not confined to only those sources shown directly "connected" in the figures.

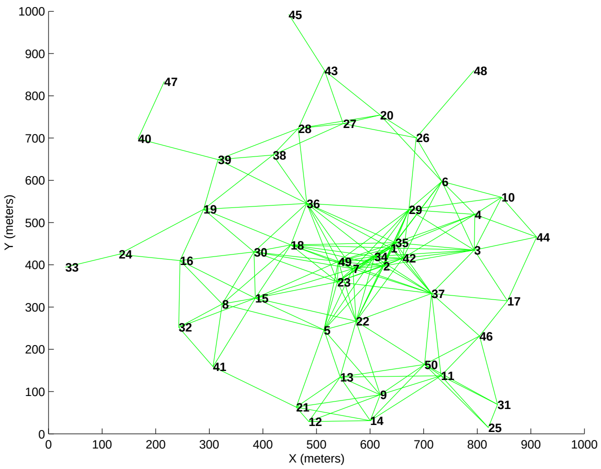

Figure 1: Network topology for the 50-node network.

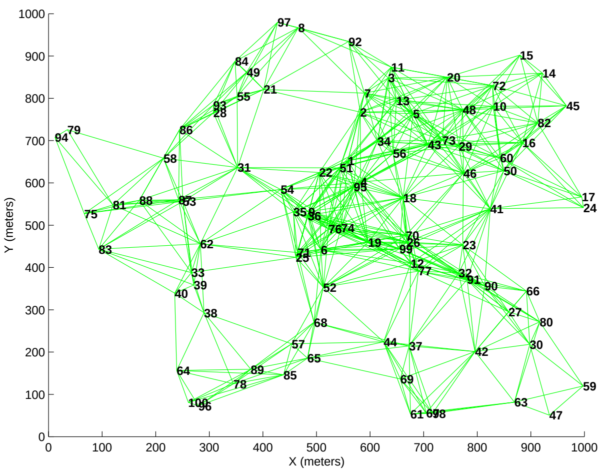

Figure 2: Network topology for the 100-node network.

Figure 3 shows the simulation and analytical results for the 50-node network. Figures 4(a) and 4(b) show the results for the 100-node network. In the graphs, the x axis contains the node ID, and the y axis shows the respective throughput. As it can be seen, the predicted performance correlates very well with practically every node in the topology (in some cases, providing very close results). In the cases where the model is off by some factor, the predicted performance follows the observed pattern in the majority of the cases.

A more statistically significant result is obtained if we

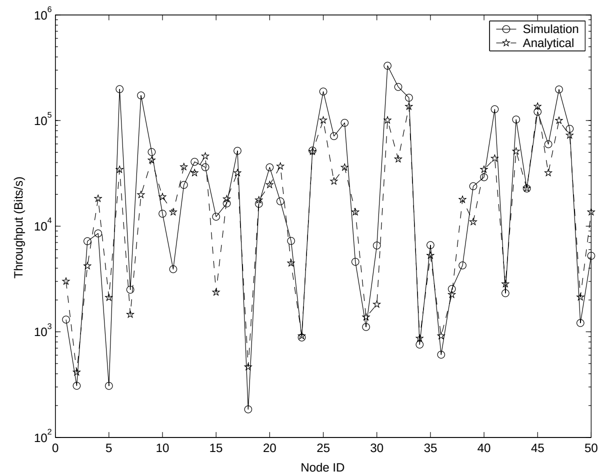

Figure 3: Throughput: simulations versus analytical model for the 50-node network.

evaluate the performance of our modeling approach over a number of different topologies. For this purpose, we considered 10 network topologies with 100 nodes each, all randomly generated as before. The topologies used for computating the histogram were similar to that shown in Fig. 2. We compute the percentage prediction error with respect to the maximum range of throughput values observed in simulations (for that particular topology) for each node in each randomly generated topology. This way, we weigh the prediction error with respect to the dynamic range of throughput values obtained in simulations. We obtained a histogram for each topology by counting the number of nodes within a certain percentage prediction error, and we then averaged the histograms over all topologies. Figure 5 shows our results. As we can see, the percentage prediction error is within 20% in about 90% of the nodes, showing how close our analytical model is in predicting the results obtained in simulations.

Finally, we show the application of our model in predicting the *average* throughput for a given network topology. For this purpose, we consider four topologies with 25, 50, 75, and 100 nodes. Figure 6 shows the comparison between the average throughput obtained in both simulations and analytical model. As we can see, the analytical model provides very good results compared to simulation results. This last figure also shows how scalable is our model in computing throughput for different network sizes and parameters.

5.3 Modeling Time

The importance of the above results and the strength of our analytical model become apparent when we analyze the time required to obtain the above results through simulation and with our analytical model. In Qualnet, *each run* of the simulation for the 100-node scenario (consisting of a 5-minute data traffic) takes about 1,118.4 seconds (19.69 minutes) in a Sun Blade 100 machine running Solaris 5.8. For the 50 seeds needed, this corresponds to 16.41 hours of simulation. In this same machine, our analytical model, implemented in Matlab 6.0, takes about 0.44 seconds. This corresponds to a time saving of more than 134,000 times. Clearly, this is a strong argument supporting the case for

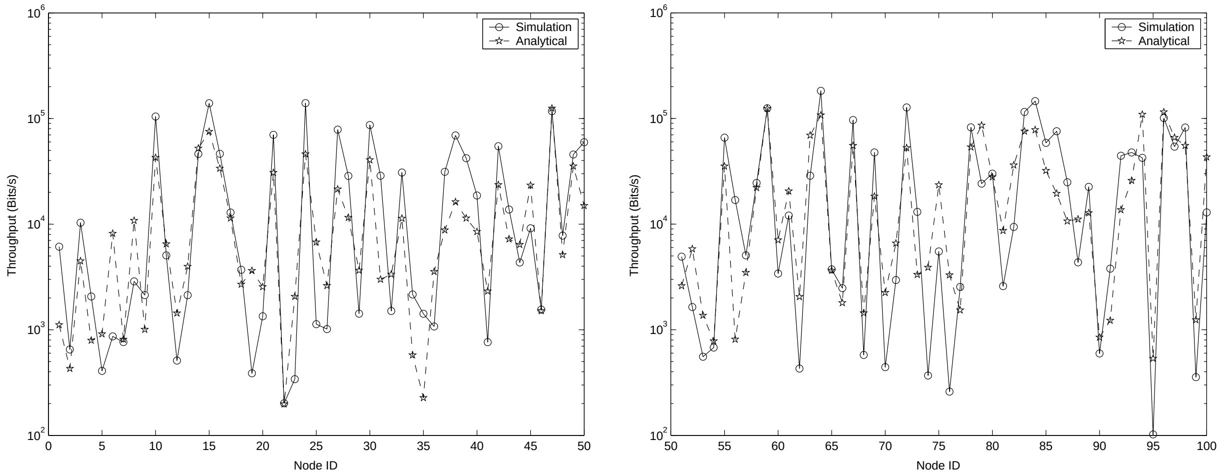

(a)

(b)

Figure 4: Throughput: simulations versus analytical model for the 100-node network. (a) First 50 nodes. (b) Last 50 nodes.

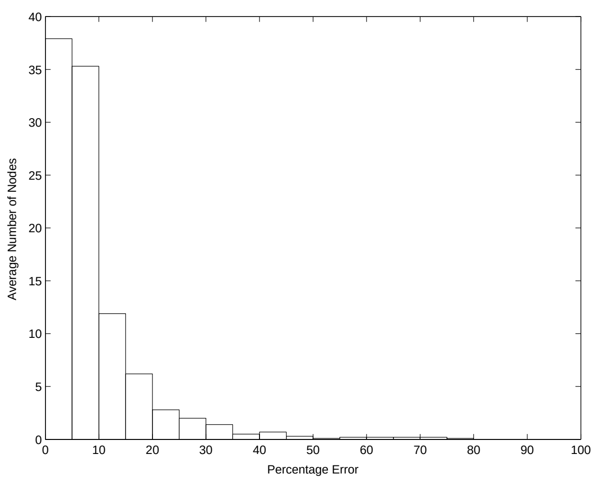

Figure 5: Percentage error prediction histogram over 10 random topologies.

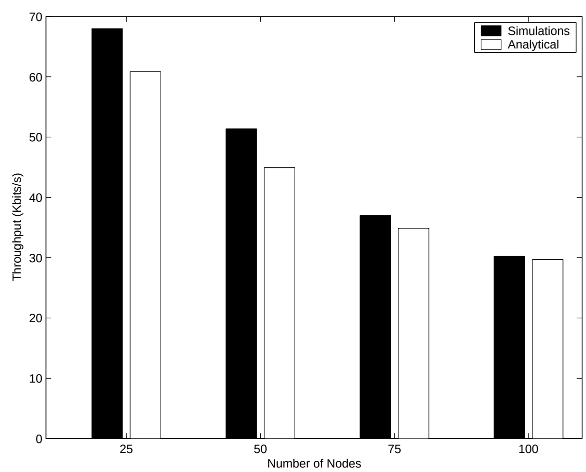

Figure 6: Average throughput for different network sizes.

the need of powerful analytical models for multihop ad hoc networks, such as the one we are providing here.

5.4 Model Limitations

The simplifications in our application of the modeling framework to the analysis of ad hoc networks using the IEEE 802.11 DCF could explain some of the disagreements between the analytical model and simulations.

In the model we first presented in [3], it is assumed that periods of collisions experienced by colliding nodes have the same duration as periods in which the channel is sensed busy by non-colliding nodes. This assumption has a direct impact on the number of nodes contending for the channel at any given time. When two or more nodes transmit at about the same time, if their packets collide, they will wait CTS_timeout seconds until they figure out that a collision has occurred. On the other hand, nodes that did not transmit at that particular time will sense a "clear channel" much earlier before colliding nodes do and, therefore, are more likely to be ready to transmit before the colliding nodes. For this reason, our model implies a more "aggressive" network, where the probability of having a node transmitting at any given time is higher than in real scenarios.

An important limitation of the model has to do with the impact of the capture effects. In the linearization procedure of Section 3, we only considered the terms corresponding to maximum SINR, which were exactly those cases where *none* of the interfering nodes were transmitting at the same time as the node under consideration. In contrast, the capture effects are present in Qualnet simulations, which are known to affect throughput performance considerably [51]. Nevertheless, the analytical model seems to capture the general trend and provide a striking correlation, even in a scenario with 100 nodes, where the contention degree and hidden terminals are significant.

Another limitation of the modeling framework introduced in Section 3 is that the interference matrix of a network corresponds to a snapshot of the transmission decisions made by the network nodes, i.e., it assumes a constant choice of a receiver by any one sender. In practice a node will choose to transmit to different neighbors or groups of neighbors. The interference matrix needs to be extended to take this effect into account.[3]

6. ADDITIONAL APPLICATION: EVALUATING THE EFFECT OF CARRIER-SENSING RANGE

Here we illustrate how our modeling framework can be applied to study different aspects of PHY and MAC layers in ad hoc networks using the IEEE 802.11 DCF. We focus on the impact of the *carrier sensing range* on network performance. In the literature, the effect of these parameters on network performance has not been treated appropriately and, more importantly, no analytical model to date has been able to deal with this problem as faithfully as our modeling framework can.

In reality, none of the PHY-layer parameters can be "set" or "adjusted" beforehand. Despite the fact that current wireless cards permit setting up specific power thresholds for both receive and sensing operations, the actual transmission and sensing ranges depend on many other factors, such as path-loss propagation (which, in turn, depends on the surrounding environment), multipath fading, transmit power, and antenna gains. However, given a radio propagation model and a specific PHY layer, we can study the impact of the carrier-sensing range using our analytical model.

In the analysis that follows, we apply the same PHY- and MAC-layer parameters used in Section 5 under the same channel conditions (no multipath fading or shadowing). The only exception is the "Sensitivity of PHY," which is a "tunable" parameter to set the sensing range in Qualnet simulations, for a given radio propagation model and PHY layer. In other words, the transmission power of each node is kept fixed (10 dBm, in our case) and the sensing range is set by changing the above threshold (this is how one would proceed in numerical simulations, too). We use the same topology depicted in Figure 2.

To study the impact of the carrier-sensing range on network performance, we hold constant the transmission range and vary the carrier sensing range of each node to obtain the corresponding throughput performance. We investigate three carrier sensing ranges: 200 m, 300 m, and 400 m. Figure 7 shows the results for the average aggregate throughput for both simulations and analytical model. As we can see, when the carrier sensing range increases, the average throughput decreases for both simulations and analytical models. One reason behind this phenomenon is that, when the carrier sensing range increases, the nodes spend more time in backoff, freezing their backoff counters more frequently as a result of being more sensitive to any activity in the channel, due to their higher sensing range. Therefore, the average service time increases and, consequently, throughput decreases.

A more intriguing behavior renders the results shown in Figure 7. The carrier sensing range is usually set to twice the transmission range to avoid some of the hidden-terminal problems, because nodes are able to sense the activity of other nodes not in their transmission range during their backoff. Therefore, when the carrier-sensing range is set to a value equal to the transmission range (in our case, 200 m), the effects of the hidden terminal problem become more apparent, because more RTS/CTS collisions happen. In simulations, this results in a high degree of unfairness, typical of the IEEE 802.11, rather than causing an average lower throughput among nodes. In fact, in simulations, a few nodes succeed in acquiring the channel when the carrier sensing range is small and, therefore, attain high throughput values, but other nodes have zero or practically null throughput. Therefore, the "average" result shown in Figure 7 for the 200-m sensing range actually refers to high throughput values (of a few nodes), averaged over all nodes. Figure 8 shows the simulation results on a per-node basis.

The analytical model we designed does not incorporate the fairness problems of the IEEE 802.11. Consequently, due to the hidden-terminal problems, nodes have lower throughput, but still transmit something. Figure 9 shows the analytical results.

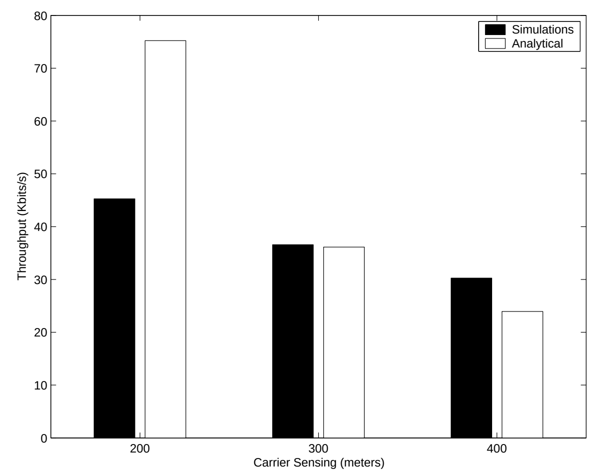

Figure 7: The impact of carrier sensing range on average network throughput.

7. CONCLUSIONS

We have introduced a novel modeling framework for multihop ad hoc networks that explicitly takes into account the impact of the PHY layer on the operation and performance of the MAC layer. A key feature of our model is that nodes can be modeled *individually*, i.e., it allows a per-node setup of many layer-specific parameters. Moreover, no spatial probability distribution or pre-arrangement of nodes is assumed. Instead, it allows the modeling of specific network topologies and radio channel models.

Our analytical model constitutes a tool for a fast, accurate, and efficient evaluation of a node's performance for any system parameter value and topology of an ad hoc network. We have illustrated this using the IEEE 802.11 DCF as an example. Attempting to characterize a node's performance only by simulations would require considerable computational effort, specially when scalability is one of the main

[3]This effort is the subject of a forthcoming publication.

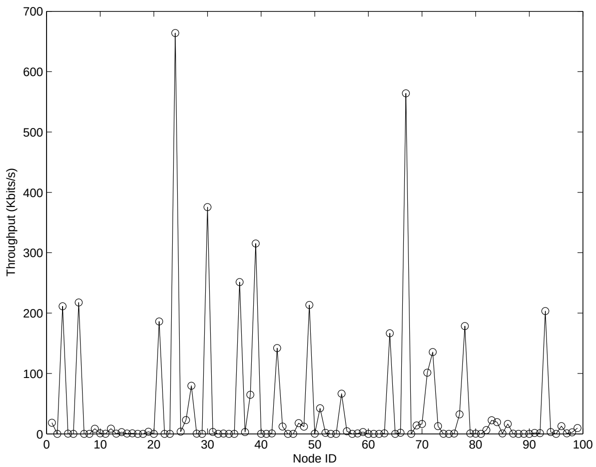

Figure 8: Average throughput for simulations when the carrier sensing range is 200m.

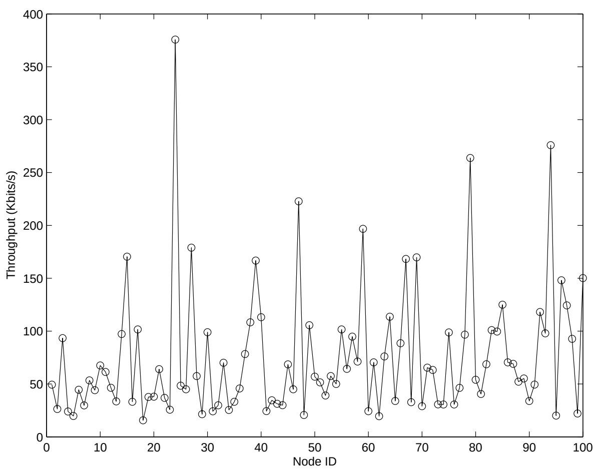

Figure 9: Average throughput for the analytical model when the carrier sensing range is 200m.

concerns. To be able to draw general conclusions, simulations would have to be run for a very large number of network sizes and topologies. Furthermore, if we are interested in evaluating the impact of a single parameter to a node's service time, for instance, simulations would have to be repeated for each parameter value of interest.

Our model was validated through discrete event simulations using the popular Qualnet tool, and the analytical results show a striking correlation with the results obtained via simulation. The importance of the analytical model is that the time needed to obtain the desired results takes a very small fraction of the time required to obtain the same results via discrete-event simulations.

Lastly, we presented the first analytical treatment of the impact of the carrier sensing range on network throughput in ad hoc networks using the IEEE 802.11 DCF. As we observed, average throughput decreases as the carrier sensing increases for a fixed transmission range. Moreover, we have noticed that the unfairness problems of the IEEE 802.11 become apparent when the carrier sensing range is equal to the transmission range, where a few nodes acquire the channel in detriment of other nodes, whose throughput is deteriorated to almost null values due to the increase of collisions from hidden terminals. The analytical model, on the other hand, produces results assuming a "fair" operation of the IEEE 802.11 DCF and, consequently, higher throughputs for that case.

8. REFERENCES

[1] R. Gallager, "A perspective on multiaccess channels," *IEEE Trans. Information Theory*, vol. IT-31, pp. 124–142, Mar 1985.

[2] A. Ephremides and B. Hajeck, "Information theory and communication networks: An unconsumated union," *IEEE Trans. Information Theory*, vol. 44, pp. 2416–2434, Oct 1998.

[3] M. M. Carvalho and J. J. Garcia-Luna-Aceves, "Delay analysis of IEEE 802.11 in single-hop networks," in *Proc. of 11th IEEE International Conference on Network Protocols (ICNP)*, Atlanta, USA, November 2003.

[4] G. Bianchi, "Performance analysis of the IEEE 802.11 distributed coordination function," *IEEE Journal on Selected Areas in Communications*, vol. 18, no. 3, pp. 535–547, March 2000.

[5] Scalable Network Technologies, Inc, *Qualnet Simulator*, Version 3.5.

[6] N. Abramson, "The ALOHA system—another alternative for computer communications," in *AFIPS Conf. Proc.* FJCC, 1970, vol. 37, pp. 281–285.

[7] N. Abramson, "The throughput of packet broadcast channels," *IEEE Trans. on Communications*, vol. COM-25, no. 1, pp. 117–128, Jan 1977.

[8] L. Kleinrock and F. A. Tobagi, "Packet switching in radio channels: Part I - carrier sense multiple-access modes and their throughput-delay characteristics," *IEEE Transactions on Communications*, vol. COM-23, no. 12, pp. 1400–1416, 1975.

[9] F. A. Tobagi and L. Kleinrock, "Packet switching in radio channels: Part II - the hidden terminal problem in carrier sense multiple-access modes and the busy-tone solution," *IEEE Transactions on Communications*, vol. COM-23, no. 12, pp. 1417–1433, 1975.

[10] L. G. Roberts, "ALOHA packet system with and without slots and capture," *Comput. Commun. Rev.*, vol. 5, pp. 28–42, Apr 1975.

[11] L. Kleinrock and S. S. Lam, "Packet switching in a multiaccess broadcast channel: Performance evaluation," *IEEE Trans. on Communications*, vol. COM-23, no. 4, pp. 410–423, Apr 1975.

[12] A. Colvin, "CSMA with collision avoidance," *Computer Commun.*, vol. 6, no. 5, pp. 227–235, 1983.

[13] W. F. Lo and H. T. Mouftah, "Carrier sense multiple access with collision detection for radio channels," in *IEEE 13th Int'l Commun. and Energy Conf.*, 1984, pp. 244–247.

[14] P. Karn, "MACA - a new channel access method for packet radio," in *ARRL/CRRL Amateur Radio 9th Computer Networking Conference*, 1990, pp. 134–140.

[15] V. Barghavan, A. Demers, S. Shenker, and L. Zhang, "MACAW: A media access protocol for wireless

LAN's," in *Proc. of ACM SIGCOMM '94*, 1994, pp. 212–225.

[16] C. L. Fullmer and J. J. Garcia-Luna-Aceves, "Floor acquisition multiple access (FAMA) for packet-radio networks," in *SIGCOMM '95*, Cambridge, MA (USA), Aug 1995, pp. 262–273.

[17] C. L. Fullmer and J. J. Garcia-Luna-Aceves, "Solutions to hidden terminal problems in wireless networks," in *Proc. ACM SIGCOMM 97*, Cannes, France, September 1997.

[18] D. Raychauduri, "Performance analysis of random access packet-switched code division multiple access systems," *IEEE Trans. Commun.*, vol. COM-29, no. 6, pp. 895–901, Jun 1981.

[19] D. H. Davis and S. A. Gronemeyer, "Performance of slotted ALOHA random access with delay capture and randomized time of arrival," *IEEE Trans. Commun.*, vol. COM-28, no. 5, pp. 703–710, May 1980.

[20] M. Musser and J. Daigle, "Throughput analysis of an asynchronous code division multiple access (CDMA) system," in *Proc. ICC'82*, Philadelphia, PA, Jun 1982.

[21] M. Pursley, "Throughput of frequency-hopped spread spectrum communications for packet radio networks," in *Proc. 1983 CISS*, John Hopkins Univ., Baltimore, MD, USA, 1983.

[22] J. C. Arnbak and W. Van Blitterswijk, "Capacity of slotted aloha in rayleigh-fading channels," *IEEE Journal on Selected Areas in Communications*, vol. SAC-5, no. 2, pp. 261–269, Feb 1987.

[23] F. Cali, M. Conti, and E. Gregori, "Dynamic tuning of the IEEE 802.11 protocol to achieve a theoretical throughput limit," *IEEE/ACM Transactions on Networking*, vol. 8, no. 6, pp. 785–799, Dec 2000.

[24] C. Foh and M. Zukerman, "Performance analysis of the IEEE 802.11 MAC protocol," in *Proc. of the European Wireless 2002 Conference*, Florence, Italy, February 2002, pp. 184–190.

[25] H. Kim and J. C. Hou, "Improving protocol capacity with model-based frame scheduling in IEEE 802.11-operated WLANs," in *Proc. of the 9th ACM International Conference on Mobile Computing and Networking (MOBICOM)*, San Diego, CA, USA, Sep 2003, pp. 190–204.

[26] Z. Hadzi-Velkov and B. Spasenovski, "The influence of flat rayleigh fading channel with hidden terminals and capture over the IEEE 802.11 WLANs," in *Proc. 54th IEEE Vehicular Technology Conference*, 2001, vol. 2, pp. 972–976.

[27] Z. Hadzi-Velkov and B. Spasenovski, "On the capacity of IEEE 802.11 DCF with capture in multipath-faded channels," *International Journal of Wireless Information Networks*, vol. 9, no. 3, pp. 191–199, July 2002.

[28] I. Gitman, "On the capacity of slotted ALOHA networks and some desigh problems," *IEEE Trans. on Communications*, vol. COM-23, no. 3, pp. 305–317, Mar 1975.

[29] F. A. Tobagi, "Analysis of a two-hop centralized packet radio network—part I: Slotted ALOHA," *IEEE Trans. Commun.*, vol. COM-28, no. 2, pp. 196–207, Feb 1980.

[30] F. A. Tobagi, "Analysis of a two-hop centralized packet radio network—part II: Carrier sense multiple access," *IEEE Trans. Commun.*, vol. COM-28, no. 2, pp. 208–216, Feb 1980.

[31] R. R. Boorstyn, A. Kershenbaum, B. Maglaris, and V. Sahin, "Throughput analysis in multihop CSMA packet radio networks," *IEEE Trans. on Communications*, vol. COM-35, no. 3, pp. 267–274, Mar 1987.

[32] F. A. Tobagi and J. M. Brazio, "Throughput analysis of multihop packet radio network under various channel access schemes," in *Proc. INFOCOM'83*, San Diego, CA, Apr 1983.

[33] T. J. Shepard, "A channel access scheme for large dense packet radio networks," in *Proc. of ACM SIGCOMM*. Aug 1996, pp. 219–230, ACM Press.

[34] H. Chhaya and S. Gupta, "Performance modeling of asynchronous data transfer methods of IEEE 802.11 MAC protocol," *Wireless Networks*, vol. 3, pp. 217–234, 1997.

[35] Y. Wang and J. J. Garcia-Luna-Aceves, "Performance of collision avoidance protocols in single-channel ad hoc networks," in *Proc. of 10th IEEE International Conference on Network Protocols (ICNP)*, Paris, France, Nov 2002.

[36] L. Wu and P. Varshney, "Performance analysis of CSMA and BTMA protocols in multihop networks (I). single channel case," *Information Sciences, Elsevier Sciences Inc.*, vol. 120, pp. 159–177, 1999.

[37] P. Gupta and P. R. Kumar, "The capacity of wireless networks," *IEEE Trans. on Information Theory*, vol. 46, no. 2, pp. 388–400, Mar 2000.

[38] M. Grossglauser and D. Tse, "Mobility increases the capacity of ad hoc wireless networks," *IEEE/ACM Trans. Networking*, vol. 10, no. 4, pp. 477–486, Aug 2002.

[39] M. Gastpar and M. Vetterli, "On the capacity of mobile ad hoc networks with delay constraints," in *Proc. of IEEEINFOCOM*, Jun 2002, vol. 3, pp. 1577–1586.

[40] S. Yi, Y. Pei, and S. Kalyanaraman, "On the capacity improvement of ad hoc wireless networks using directional antennas," in *Proc. ACM MobiHoc*, Annapolis, USA, Jun 2003, pp. 108–116.

[41] C. Peraki and S. Servetto, "On the maximum stable throughput problem in random networks with directional antennas," in *Proc. ACM MobiHoc*, Annapolis, USA, Jun 2003, pp. 76–87.

[42] S. Toumpis and A. J. Goldsmith, "Capacity regions for wireless ad hoc networks," *IEEE Trans. Wireless Communications*, vol. 2, no. 4, pp. 736–748, Jul 2003.

[43] R. Moraes, H. Sadjadpour, and J. J. Garcia-Luna-Aceves, "Making ad-hoc networks scale using mobility and multi-copy forwarding," in *Proc. of IEEE Globecom*, Nov 2004, To appear.

[44] A. El Gamal, E. Uysal, and B. Prabhakar, "Energy-efficient transmission over a wireless link via lazy packet scheduling," in *Proc. of IEEE INFOCOM*, Apr 2001, vol. 1, pp. 386–394.

[45] A. Fu, E. Modiano, and J. Tsitsiklis, "Transmission scheduling over a fading channel with energy and deadline constraints," in *Proc. Conference on Information Sciences and Systems*, Mar 2002.

[46] L. Tong, Q. Zhao, and G. Mergen, “Multipacket reception in random access wireless networks: From signal processing to optimal medium access control,” *IEEE Commun. Mag.*, vol. 39, no. 12, pp. 108–112, 2001.

[47] A. Maharshi, L. Tong, and A. Swami, “Cross-layer designs of multichannel reservation mac under rayleigh fading,” *IEEE/ACM Trans. Signal Processing*, vol. 51, no. 8, pp. 2054–2067, Aug 2003.

[48] M. Zorzi, “Mobile radio slotted ALOHA with capture, diversity and retransmission control in the presence of shadowing,” *Wireless Networks*, vol. 4, pp. 379–388, Aug 1998.

[49] J. H. Kim and J. K. Lee, “Capture effects of wireless csma/ca protocols in rayleigh and shadow fading channels,” *IEEE Trans. Veh. Tech.*, vol. 48, no. 3, pp. 1277–1286, Mar 1999.

[50] Gordon L. Stuber, *Principles of Mobile Communication*, Kluwer Academic Publishers, 2000.

[51] C. T. Lau and C. Leung, “Capture models for mobile packet radio networks,” *IEEE Transactions on Communications*, vol. 40, no. 5, pp. 917–925, May 1992.

[52] F. A. Tobagi, “Modeling and performance analysis of multihop packet radio networks,” *Proc. IEEE*, vol. 75, no. 1, pp. 135–155, Jan 1987.

[53] *IEEE Standard for Wireless LAN Medium Access Control (MAC) and Physical Layer (PHY) Specifications*, Nov 1997, P802.11.

[54] S. J. Oh and K. M. Wasserman, “Dynamic spreading gain control in multiservice CDMA networks,” *IEEE Journal on Selected Areas in Communications*, vol. 17, no. 5, pp. 918–927, 1999.

[55] D. Tse and S. Hanly, “Linear multiuser receivers: Effective interference, effective bandwidth and user capacity,” *IEEE Trans. Information Theory*, vol. 45, no. 2, pp. 641–657, Mar 1999.

[56] G. H. Golub and C. F. Van Loan, *Matrix Computations*, The John Hopkins University Press, third edition, 1996.